Coupling of the Plasmon Resonances of Chemically Functionalized Gold Nanoparticles to Local Order in Thermotropic Liquid Crystals

Gary M. Koenig Jr., Maria-Victoria Meli, Joon-Seo Park, Juan J. de Pablo, and Nicholas L. Abbott*

Department of Chemical and Biological Engineering, University of Wisconsin−Madison, 1415 Engineering Drive, Madison, Wisconsin 53706

Received October 12, 2006. Revised Manuscript Received December 21, 2006

We report that surface-induced ordering of liquid crystals in the vicinity of chemically functionalized gold nanoparticles leads to changes in the localized surface plasmon resonance (LSPR) of the gold nanoparticles. Gold nanoparticles with sizes between 10 and 40 nm were prepared on surfaces and chemically functionalized with organic monolayers that are known to lead to planar and homeotropic orientations of micrometer-thick films of nematic 4-pentyl-4′cyanobiphenyl (5CB) supported on continuous gold films. By measuring the absorption of light caused by the LSPR of the nanoparticles as a function of surface chemistry of the nanoparticles and temperature, we observed changes in the LSPR caused by surface-induced, localized ordering of the 5CB in the vicinity of the nanoparticles. Comparison of the far-field orientation of the liquid crystal and the LSPR behavior of the nanoparticles provides insights into the nanoscopic origins of the bulk anchoring behaviors of the liquid crystal. These results and others presented in this paper indicate that the LSPR properties of nanoparticles can be exploited to investigate how the chemical functionality of nanoparticles changes the local ordering of liquid crystals.

Introduction

Recent theories and simulations have investigated topological defects that form around individual spherical particles[1−8] dispersed in liquid crystalline solvents as well as interactions between particles dispersed in (i) nematic phases[9−12] and (ii) isotropic phases prepared by the heating of nematic phases.[13−18] Whereas the topological defects that form about micrometer-sized particles in liquid crystals have been characterized by using optical microscopy,[19−29] few experimental methods exist to probe the ordering of liquid crystals about nanoscopic particles. Recent calculations suggest that the surface plasmons of metal nanoparticles in anisotropic media such as liquid crystals are strongly dependent on the local ordering of the liquid crystal[30,31] and that electric field-induced orientational transitions of the liquid crystal may be used to tune the optical properties of metal nanoparticles.[32] In this paper, we report a first step toward developing methods based on the optical properties of metallic nanoparticles to investigate the influence of surface chemistry on the ordering of liquid crystals in the vicinity of the nanoparticles. We report that manipulation of the surface chemistry of gold nanoparticles does lead to changes in the local ordering of a liquid crystal in the vicinity of the nanoparticles, as reported by the changes in the localized surface plasmon resonance (LSPR) of the nanoparticles.

The optical properties of gold and other noble metal nanoparticles have been extensively investigated in recent

* To whom correspondence should be addressed. Tel: (608) 265-5278. Fax: (608) 262-5434. E-mail: abbott@engr.wisc.edu.

(1) Vitelli, V.; Turner, A. M. *Phys. Rev. Lett.* **2004**, *93*, 215301.
(2) Fukuda, J.-I.; Yoneya, M.; Yokoyama, H. *Phys. Rev. E* **2002**, *65*, 41709.
(3) Grollau, S.; Abbott, N. L.; de Pablo, J. J. *Phys. Rev. E* **2003**, *67*, 51703.
(4) Stark, H.; Ventzki, D. *Phys. Rev. E* **2001**, *64*, 31711.
(5) Andrienko, D.; Germano, G.; Allen, M. P. *Phys. Rev. E* **2001**, *63*, 41701.
(6) Ruhwandl, R. W.; Terentjev, E. M. *Phys. Rev. E* **1997**, *56*, 5561.
(7) Ruhwandl, R. W.; Terentjev, E. M. *Phys. Rev. E* **1996**, *54*, 5204.
(8) Kuksenok, O. V.; Ruhwandl, R. W.; Shiyanovskii, S. V.; Terentjev, E. M. *Phys. Rev. E* **1996**, *54*, 5198.
(9) Guzman, O.; Kim, E. B.; Grollau, S.; Abbott, N. L.; de Pablo, J. J. *Phys. Rev. Lett.* **2003**, *91*, 235507.
(10) Araki, T.; Tanaka, H. *J. Phys.: Condensed Matter* **2006**, *18*, 193.
(11) Fukuda, J.-I.; Yoneya, M.; Yokoyama, H.; Stark, H. *Colloids Surf., B* **2004**, *38*, 143−147.
(12) Fukuda, J.-I.; Stark, H.; Yoneya, M.; Yokoyama, H. *Phys. Rev. E* **2004**, *69*, 41706.
(13) Fukuda, J.-I.; Stark, H.; Yokoyama, H. *Phys. Rev. E* **2005**, *72*, 21701.
(14) Stark, H.; Fukuda, J.-I.; Yokoyama, H. *Phys. Rev. Lett.* **2004**, *92*, 205502.
(15) Stark, H. *Phys. Rev. E* **2002**, *66*, 41705.
(16) Borstnik, A.; Stark, H.; Zumer, S. *Phys. Rev. E* **2000**, *61*, 2831.
(17) Borstnik, A.; Stark, H.; Zumer, S. *Phys. Rev. E* **1999**, *60*, 4210.
(18) Galatola, P.; Fournier, J. B. *Phys. Rev. Lett.* **2001**, *86*, 3915.
(19) Poulin, P.; Stark, H.; Lubensky, T. C.; Weitz, D. A. *Science* **1997**, *275*, 1770.
(20) Loudet, J.-C.; Barois, P.; Poulin, P. *Nature* **2000**, *407*, 611.
(21) Poulin, P.; Weitz, D. A. *Phys. Rev. E* **1998**, *57*, 626.
(22) Poulin, P.; Cabuil, V.; Weitz, D. A. *Phys. Rev. Lett.* **1997**, *79*, 4862.
(23) Loudet, J. C.; Poulin, P. *Phys. Rev. Lett.* **2001**, *87*, 165503.
(24) Gu, Y.; Abbott, N. L. *Phys. Rev. Lett.* **2000**, *85*, 4719.
(25) Liao, G.; Smalyukh, I. I.; Kelly, J. R.; Lavrentovich, O. D.; Jakli, A. *Phys. Rev. E* **2005**, *72*, 31704.
(26) Noel, C. M.; Bossis, G.; Chaze, A. M.; Giulieri, F.; Lacis, S. *Phys. Rev. Lett.* **2006**, *96*, 217801.
(27) Skarabot, M.; Ravnik, M.; Babic, D.; Osterman, N.; Poberaj, I.; Zumer, S.; Musevic, I.; Nych, A.; Ognysta, U.; Nazarenko, V. *Phys. Rev. E* **2006**, *73*, 21705.
(28) Kossyrev, P.; Ravnik, M.; Zumer, S. *Phys. Rev. Lett.* **2006**, *96*, 48301.
(29) Smalyukh, I. I.; Kuzmin, A. N.; Kachynski, A. V.; Prasad, P. N.; Lavrentovich, O. D. *Appl. Phys. Lett.* **2005**, *86*, 21913.
(30) Park, S. Y.; Stroud, D. *Appl. Phys. Lett.* **2004**, *85*, 2920.
(31) Park, S. Y.; Stroud, D. *Phys. Rev. Lett.* **2005**, *94*, 217401.
(32) Lawandy, N. M.; Smuk, A. Y. *J. Soc. Information Display* **2005**, *13*, 755.

10.1021/cm062438p CCC: $37.00
Published on Web 02/13/2007

years.[33−39] The collective oscillation of the conduction electrons for noble metal particles in the 10−200 nm size range leads to a peak in the visible range of the absorption spectrum of the nanoparticles.[33,39] This peak in absorbance results in the nanoparticles exhibiting brilliant colors. The wavelength of the peak absorption is known to depend on the dielectric environment of the nanoparticle.[38] An increase in the refractive index of the medium surrounding the nanoparticle results in a red-shift in the wavelength of the absorption maximum.[40,41] For gold nanoparticles supported on glass substrates, LSPR has been shown to be sensitive to changes in the dielectric environment within 20 nm of the nanoparticle surface.[42] In the study reported in this paper, the dielectric environment of the nanoparticles is influenced by the ordering of a liquid crystal in the vicinity of the nanoparticles.

The liquid crystal used in our study is 4-pentyl-4′cyanobiphenyl (5CB). In the bulk, this material displays a crystalline phase below 24 °C,[43] a nematic liquid crystalline phase from 24 to 33.5 °C, and an isotropic liquid phase above 33.5 °C.[44] The orientational ordering of molecules within the nematic phase leads to anisotropic dielectric properties. For example, at room temperature, the extraordinary and ordinary refractive indices of the bulk nematic phase of 5CB differ by 0.18.[44] The large anisotropy in the bulk dielectric properties of the liquid crystal led us to predict that the surface plasmons of nanoparticles in liquid crystals may provide a convenient means to probe changes in the ordering of liquid crystals that have been predicted to occur near the surfaces of nanoparticles.[45] We note that several prior studies have addressed the influence of liquid crystals on surface plasmon resonance (SPR) phenomena. For example, SPR microscopy[46] and reflectance spectroscopy[47] have been used to investigate the impact of the orientation of a liquid crystal on the surface plasmon resonance of continuous metal films. Electric field-induced orientational transitions of liquid crystals have also been used to control the reflectance of continuous metal films[48−51] and the scattering of light from individual[52] and arrays[53] of metallic nanoparticles. These past studies have not investigated the influence of the chemistry of nanoparticles on surface-induced ordering of liquid crystals with the goal of exploiting LSPR behavior to provide insight into the coupling between surface chemistry and local order in the liquid crystal.

Several recent studies have investigated the dielectric properties of dispersions of nanoparticles in liquid crystals.[54,55] For example, the addition of ferroelectric nanoparticles to liquid crystals has been shown to cause an increase in the anisotropy of the dielectric properties of the bulk material.[55] The addition of ferroelectric nanoparticles has also been shown to decrease the voltage required to cause a Fredericksz transition in a liquid crystal.[56] Studies of the effects of the concentration of nanoparticles have been reported,[57] and these studies reveal that it can be difficult to uniformly disperse nanoparticles within the bulk of liquid crystals.[58] Dispersions of nanoparticles have been reported in liquid crystal−polymer matrices,[59] discotic liquid crystals,[60] and cholesteric liquid crystals.[61] Of particular relevance to the current study, gold nanoparticles have been dispersed into discotic liquid crystals.[60] The particles used in this past study possessed a diameter of 1.6 nm, which is too small to lead to significant LSPR effects in the visible region of the absorption spectrum.

Our study used gold nanoparticles supported on a macroscopic surface. Although our initial measurements used nanoparticles dispersed into the bulk of a liquid crystal, particle−particle interactions mediated by the liquid crystal complicated our interpretation of the optical properties of the nanoparticles. These observations caused us to reduce the degrees of freedom in our experimental system by using gold nanoparticles immobilized on surfaces such that the particle−particle separation did not change as a function of ordering of the liquid crystal in the vicinity of the particles. To control the surface-induced ordering of the liquid crystals in the vicinity of the gold nanoparticles, we chemically functionalized the surfaces of the nanoparticles with self-assembled monolayers (SAMs) formed from alkanethiols. Previous studies have demonstrated that the structures of SAMs can be manipulated to achieve control over the orientation of the liquid crystal 5CB at the surfaces of alkanethiol-derivatized films of gold.[62−65] For example, a single component SAM formed from an alkanethiol (e.g., decanethiol or hexadecanethiol) will cause planar (parallel)

(33) Kreibig, U.; Vollmer, M. *Optical Properties of Metal Clusters*; Springer: Berlin, 1995.
(34) Link, S.; El-Sayed, M. A. *Ann. Rev. Phys. Chem.* **2003**, *54*, 331.
(35) Pasquato, L.; Pengo, P.; Scrimin, P. *J. Mater. Chem.* **2004**, *14*, 3481.
(36) Elghanian, R.; Storhoff, J. J.; Mucic, R. C.; Letsinger, R. L.; Mirkin, C. A. *Science* **1997**, *277*, 1078.
(37) Sun, Y.; Xia, Y. *Science* **2002**, *298*, 2176.
(38) Kelly, K. L.; Coronado, E.; Zhao, L. L.; Schatz, G. C. *J. Phys. Chem. B* **2003**, *107*, 668.
(39) Haes, A. J.; Haynes, C. L.; McFarland, A. D.; Schatz, G. C.; van Duyne, R. P.; Zou, S. *MRS Bull.* **2005**, *30*, 368.
(40) Underwood, S.; Mulvaney, P. *Langmuir* **1994**, *10*, 3427.
(41) Haes, A. J.; Van Duyne, R. P. *Expert Rev. Mol. Diagnostics* **2004**, *4*, 527.
(42) Haes, A. J.; Zou, S.; Schatz, G. C.; Van Duyne, R. P. *J. Phys. Chem. B* **2004**, *108*, 109.
(43) Date, M.; Takeuchi, Y.; Kato, K. *J. Phys. D* **1998**, *31*, 2225.
(44) Li, J.; Gauza, S.; Wu, S.-T. *J. Appl. Phys.* **2004**, *96*, 19.
(45) Barmentlo, M.; Hollering, R. W. J.; van Aerle, N. A. J. M. *Phys. Rev. A* **1992**, *46*, 4490.
(46) Evans, S. D.; Allinson, H.; Boden, N.; Flynn, T. M.; Henderson, J. R. *J. Phys. Chem. B* **1997**, *101*, 2143.
(47) Kieser, B.; Pauluth, D.; Gauglitz, G. *Anal. Chim. Acta* **2001**, *434*, 231.
(48) Wang, Y. *Appl. Phys. Lett.* **1995**, *67*, 2759.
(49) Wang, Y.; Russell, S. D.; Shimabukuro, R. L. *J. Appl. Phys.* **2005**, *97*, 23708.
(50) Caldwell, M. E.; Yeatman, E. M. *Appl. Opt.* **1992**, *31*, 3880.
(51) Schildkraut, J. S. *Appl. Opt.* **1988**, *27*, 4587.
(52) Muller, J.; Sonnichsen, C.; von Poschinger, H.; von Plessen, G.; Klar, T. A.; Feldmann, J. *Appl. Phys. Lett.* **2002**, *81*, 171.
(53) Kossyrev, P. A.; Yin, A.; Cloutier, S. G.; Cardimona, D. A.; Huang, D.; Alsing, P. M.; Xu, J. M. *Nano Lett.* **2005**, *5*, 1978.
(54) Ouskova, E.; Buchnev, O.; Reshetnyak, V.; Reznikov, Y.; Kresse, H. *Liq. Cryst.* **2003**, *30*, 1235−1239.
(55) Reznikov, Y.; Buchnev, O.; Tereshchenko, O.; Reshetnyak, V.; Glushchenko, A.; West, J. *Appl. Phys. Lett.* **2003**, *82*, 1917.
(56) Reshetnyak, V. Y.; Shelestiuk, S. M.; Sluckin, T. J. *Mol. Cryst. Liq. Cryst.* **2006**, *454*, 603.
(57) Kobayashi, S.; Miyama, T.; Nishida, N.; Sakai, Y.; Shiraki, H.; Shiraishi, Y.; Toshima, N. *J. Display Technol.* **2006**, *2*, 121.
(58) Shiraishi, Y.; Sano, S.; Baba, A.; Kobayashi, S.; Toshima, N. *Kobunshi Ronbunshu* **2002**, *59*, 753.
(59) Yaroshchuk, O. V.; Dolgov, L. O.; Kiselev, A. D. *Phys. Rev. E* **2005**, *72*, 51715.
(60) Kumar, S.; Lakshminarayanan, V. *Chem. Commun.* **2004**, *14*, 1600.
(61) Mitov, M.; Portet, C.; Bourgerette, C.; Snoeck, E.; Verelst, M. *Nature Mater.* **2002**, *1*, 229.

anchoring of 5CB on a continuous film of gold.[62,64] However, a mixed monolayer formed from long and short alkanethiols can cause homeotropic (perpendicular) alignment of 5CB.[62−64]

Materials and Methods

Materials. 1-Hexadecanethiol, 1-decanethiol, and octyltrichlorosilane were purchased from Aldrich and used as received. Absolute ethanol was obtained from AAPER Alcohol. The liquid crystal 4-pentyl-4′cyanobiphenyl (5CB) was purchased from EMD Chemicals. Glass microscope slides, hydrochloric acid, potassium hydroxide, *n*-heptane, methylene chloride, and hydrogen peroxide were purchased from Fisher.

Substrate Cleaning. The glass microscope slides were cleaned sequentially with an acidic piranha solution (70% H_2SO_4, 30% H_2O_2) and a basic piranha solution (70% KOH, 30% H_2O_2). ***Caution!*** *The piranha solution is extremely dangerous and should be handled with caution; in some circumstances, most commonly when it has been mixed with a significant amount of oxidizable organic material, it has detonated unexpectedly.* Slides were rinsed with 18.2 MΩ deionized water, ethanol, and methanol and dried under a stream of gaseous nitrogen. Slides were stored at 110 °C for 1 day before gold deposition.

Formation of Immobilized Gold Nanoparticles. The method used to form the arrays of immobilized gold nanoparticles was adapted from procedures reported in the literature.[66,67] Gold was deposited onto cleaned glass microscope slides by electron beam evaporation (thickness of 50 Å). The deposition was performed at 2×10^{-6} Torr and a rate of 0.2 Å/s. The gold films were then annealed at 560 °C for 1 h. Atomic force microscopy (AFM) of the resulting gold nanoparticles was used to characterize the nanoparticle size, shape, and distribution on the surface. AFM imaging was performed using a Digital Instruments Multimode AFM (Nanoscope IIIA), using a Si cantilever ($f_o = \sim$300 kHz, Veeco Probes) in tapping mode. The microscope slides supporting the gold nanoparticles were visibly pink and homogeneous to the naked eye.

Formation of SAMs. SAMs were formed on the nanoparticle-decorated slides by immersing the slides in ethanolic solutions containing 4 mM alkanethiol. Three different solutions were used in our study: a solution of hexadecanethiol, a solution of decanethiol, and a solution containing an 8:2 mixture of decanethiol and hexadecanethiol. The SAMs were allowed to form overnight. Upon removal from the ethanolic alkanethiol solutions, the samples were rinsed with ethanol and dried under a stream of gaseous nitrogen. The slides remained uniform in appearance, indicating that the particles did not aggregate macroscopically on the glass surface during the previously described procedure.

Preparation of OTS-Treated Glass. Piranha-cleaned microscope slides were coated with octyltrichlorosilane (OTS) by immersion in a 10 mM solution of OTS in *n*-heptane for 30 min. The OTS functionalized glass was removed from the *n*-heptane solution, rinsed with methylene chloride, and dried under a flowing stream of gaseous nitrogen.

Preparation of Optical Cells. Optical cells were prepared by pairing OTS-treated glass with a glass slide coated with the alkanethiol functionalized nanoparticles. The two surfaces were spaced apart by using a 50 μm thick Mylar spacer. Nematic 5CB was drawn into the optical cell by capillary action. OTS-treated glass orients the liquid crystal 5CB in a homeotropic orientation at the top surface of the optical cell.[68] Prior to UV−vis spectrophotometry, the optical cells were placed in an oven at 36 °C for 30 min and then removed and allowed to cool to room temperature in ambient air.

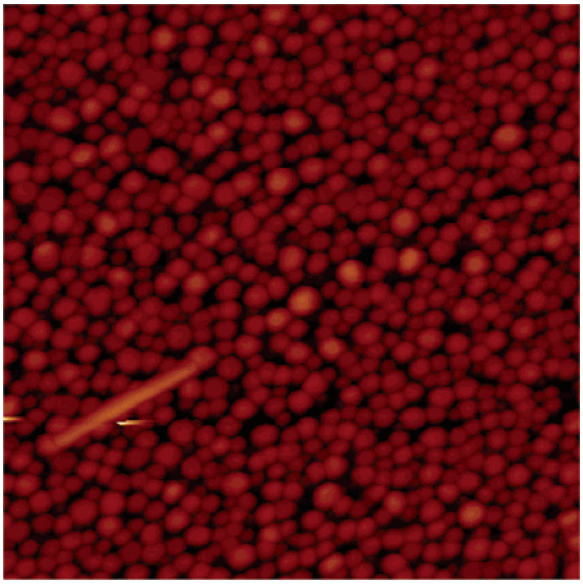

Figure 1. AFM image (1 μm × 1 μm) of gold nanoparticles used in our study.

UV−Vis Spectroscopy. UV−vis spectra of the samples were obtained by using a Cary 1E UV−vis spectrophotometer. The temperature was controlled within ±0.1 °C using a heat bath that circulated water through cuvette holders. The temperature was measured using a thermocouple placed next to the sample. The wavelength of peak absorbance due to the LSPR was determined by fitting a second-order polynomial to the experimental data points, in 0.5 nm intervals, within 10 nm of the maximum absorbance. Five scans were recorded and averaged at each temperature. The standard deviation was typically less than 0.1 nm. Data presented next show the wavelength at peak absorbance as a function of temperature. These data were collected by heating the optical cell containing 5CB to a temperature (39.3 °C) above the isotropic−nematic transition of 5CB and then slowly cooling the sample while recording the wavelength at peak absorbance as a function of temperature until a temperature well below the isotropic−nematic transition was reached (typically 26.7 °C). This procedure was then repeated in reverse, going from 26.7 to 39.3 °C. The data shown in this paper correspond to data collected during the second ramp in temperature. To assess the reversibility of the localized ordering of the 5CB near the nanoparticles, we also recorded the wavelength at peak absorbance at 30.2, 39.3, 48.4, and then 30.2 °C.

Results and Discussion

Surfaces decorated with gold nanoparticles were prepared by evaporation of gold onto a substrate and subsequent thermal annealing.[66,67] Inspection of the atomic force micrograph shown in Figure 1 reveals that the gold nanoparticles used in our experiments have apparent lateral dimensions of 32 ± 6 nm and heights of 17 ± 4 nm, although the

(62) Gupta, V. K.; Abbott, N. L. *Science* **1997**, *276*, 1533.
(63) Ruths, M.; Heuberger, M.; Scheumann, V.; Hu, J.; Knoll, W. *Langmuir* **2001**, *17*, 6213.
(64) Drawhorn, R. A.; Abbott, N. L. *J. Phys. Chem.* **1995**, *99*, 16511.
(65) Miller, W. J.; Abbott, N. L. *Langmuir* **1997**, *13*, 7106.
(66) Orfanides, P.; Buckner, T. F.; Buncick, M. C.; Meriaudeau, F.; Ferrell, T. L. *Am. J. Phys.* **2000**, *68*, 936.
(67) Kalyuzhny, G.; Vaskevich, A.; Schneeweiss, M. A.; Rubinstein, I. *Chem.−Eur. J.* **2002**, *8*, 3849.
(68) Nazarenko, V. G.; Klouda, R.; Lavrentovich, O. D. *Phys. Rev. E* **1998**, *57*, 36.

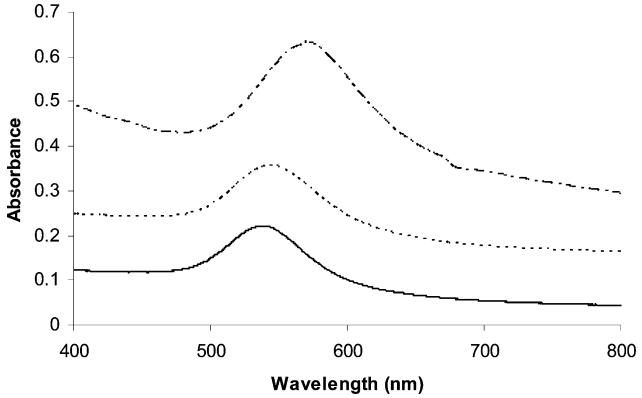

Figure 2. UV−vis absorbance spectra of gold nanoparticles shown in Figure 1: (solid, bottom line) measured in air prior to functionalization with hexadecanethiol; (dotted, middle line) measured in air after functionalization with a monolayer of hexadecanethiol; (dashed, top line) measured in nematic 5CB after functionalization with a monolayer of hexadecanethiol. The spectra are offset for clarity.

sizes of the grains in Figure 1 may also be influenced by the details of the shape of the tip of the AFM probe (tip convolution effects).[69] A past study has described the shapes of gold nanoparticles produced by thermal annealing of gold films as corresponding to oblate ellipsoids.[66] Inspection of Figure 1 also reveals that the interparticle spacing is very small and that many nanoparticles are separated from their nearest neighbor by a distance that is less than a particle diameter. The close packing of these nanoparticles suggests that the electric fields of the nanoparticles will be coupled.[70] When measured in air, the gold nanoparticle assemblies shown in Figure 1 exhibited a peak in their optical absorption spectrum at a wavelength of incident light of 538.1 nm (Figure 2). The sizes of nanoparticles produced by the previously described method, and the associated surface plasmon properties of these ensembles of nanoparticles, are influenced by the temperature and time of the thermal annealing (we measured the absorbance maximum to vary from 535 to 550 nm). The results described in this paper were obtained from two batches of nanoparticles, the first having a peak absorbance at 546.7 nm and the second having a peak absorbance at 538.1 nm (Table 1).

Prior to performing experiments with liquid crystals, we confirmed several previous observations: (i) that formation of SAMs of alkanethiols on the surfaces of these arrays of gold nanoparticles leads to changes in the wavelength of incident light at which the maximum absorbance was observed (see Figure 2 for the effect of a SAM formed from hexadecanethiol)[71] and (ii) that immersion of the SAM coated gold nanoparticles into solvents of increasing refractive index leads to systematic changes in the LSPR properties of the ensembles of gold nanoparticles.[40,72] The results of these confirmatory experiments are described in the Supporting Information. Here, we mention only that the gold nanoparticles used in our experiments, when coated with SAMs formed from hexadecanethiol, responded to changes in isotropic solvent environments by exhibiting shifts in the position of the absorbance peak of 28 nm per refractive index unit (RIU) of the solvents. Nanoparticles coated with SAMs formed from butanethiol, however, exhibited a sensitivity of 40 nm/RIU. Similar behaviors have been reported by Van Duyne and co-workers.[71]

We first investigated the influence of the ordering of 5CB on the LSPR properties of gold nanoparticles functionalized with SAMs formed from hexadecanethiol. These initial studies were based on gold nanoparticles that exhibited a maximum absorbance due to LSPR effects at 546.7 nm (see the following discussion for experiments with gold nanoparticles with LSPR peak absorbance at 538.1 nm). As mentioned previously, past studies have established that SAMs of hexadecanethiol formed on continuous gold films cause micrometer-thick films of nematic 5CB to be anchored parallel to the surface.[64] We observed surfaces presenting arrays of gold nanoparticles functionalized with SAMs formed from hexadecanethiol to also cause micrometer-thick films of the liquid crystal to assume orientations that were parallel to the macroscopic surfaces supporting the gold nanoparticles (see Supporting Information). We note that the orientation of the liquid crystal mentioned in the previous text refers to the orientation far (micrometers) from the surface supporting the nanoparticles. This far-field orientation of the liquid crystal is a consequence of local interactions of the liquid crystal with both the nanoparticles and the glass exposed between the nanoparticles. As reported in past studies of surfaces patterned with nanoscopic islands of materials that give rise to competing orientations of liquid crystals, the uniform orientation of the liquid crystal adopted far from such surfaces reflects a minimization of the free energy of the entire system, including contributions from the elastic energy stored in the liquid crystal.[73,74]

We observed initial contact of the hexadecanethiol coated gold nanoparticles with 5CB at room temperature to lead to a red-shift of the LSPR peak by 27.1 nm (from 553.7 to 580.8 nm). Inspection of Figure 3a reveals that the wavelength of the LSPR peak changed little between 26 and 33.2 °C, at which point the LSPR peak abruptly red-shifted by an additional 0.9 nm. This abrupt transition coincides within our experimental precision to the temperature of the bulk nematic-to-isotropic transition, suggesting that there is a coupling between the order in the 5CB and the LSPR of these chemically functionalized gold nanoparticles. We note that the published value of the clearing temperature of 5CB is 33.5 °C.[44] The value reported in Figure 3a is 0.3 °C lower than the published value. This difference is due to a systematic offset in the temperature of the thermocouple used to measure the temperature of our experimental system. Above 33.2 °C, we measured the LSPR peak to change little with temperature, consistent with the weak temperature dependence of the refractive index above the clearing temperature.[44] This weak temperature dependence of the refractive index of 5CB in the isotropic phase can be seen

(69) Tabet, M. F.; Urban, F. K., III. *J. Vac. Sci. Technol., B* **1997**, *15*, 800.
(70) Rechberger, W.; Hohenau, A.; Leitner, A.; Krenn, J. R.; Lamprecht, B.; Aussenegg, F. R. *Opt. Commun.* **2003**, *220*, 137.
(71) Malinsky, M. D.; Kelly, K. L.; Schatz, G. C.; Van Duyne, R. P. *J. Am. Chem. Soc.* **2001**, *123*, 1471.
(72) Jensen, T. R.; Duval, M. L.; Kelly, K. L.; Lazarides, A. A.; Schatz, G. C.; Van Duyne, R. P. *J. Phys. Chem. B* **1999**, *103*, 9846.
(73) Zhang, B.; Lee, F. K.; Tsui, O. K. C.; Sheng, P. *Phys. Rev. Lett.* **2003**, *91*, 215501.
(74) Ong, H. L.; Hurd, A. J.; Meyer, R. B. *J. Appl. Phys.* **1985**, *57*, 186.

Table 1. Wavelength at Peak Absorbance for Immobilized Gold Nanoparticles[a]

Alkanethiol used for chemical functionalization of gold nanoparticles	Wavelength at peak absorbance, measured in air prior to chemical functionalization (nm)	Wavelength at peak absorbance, measured in air after chemical functionalization (nm)	Red-shift in peak absorbance caused by formation of monolayer on surface of nanoparticles (nm)	Wavelength at peak absorbance, measured in liquid crystal after chemical functionalization (nm)	Red-shift in peak absorbance upon immersion into liquid crystal (nm)
Decanethiol	546.7	550.2	3.5	582.6	32.4
Hexadecanethiol	546.9	553.7	6.8	580.8	27.1
Mixed monolayer of decanethiol and hexadecanethiol	546.5	551.8	5.3	579.7	27.1
Decanethiol	538.2	540.0	1.8	567.8	27.8
Hexadecanethiol	538.1	544.1	6.0	569.6	25.5
Mixed monolayer of decanethiol and hexadecanethiol	538.1	541.8	3.7	569.7	27.9

[a] (i) In air, prior to chemical functionalization with the alkanethiol indicated in the far left column of the table, (ii) in air, after chemical functionalization with alkanethiol, and (iii) in nematic 5CB at 30.2 °C after chemical functionalization with the alkanethiol. Also indicated in the table is the red-shift in the peak absorbance caused by (i) formation of the alkanethiol monolayer (measurements in air, column 4) and (ii) immersion into nematic 5CB from air (column 6).

in Figure 4, where the ordinary and extraordinary refractive indices have collapsed to a single value that decreases only slightly with increase in temperature. Repeated cycling of the temperature between 30.2 and 39.3 °C resulted in reproducible changes in the positions of the maximum absorbance caused by the LSPR phenomenon (Figure 3b). As shown in Figure 3b, an excursion in temperature to 48.4 °C leads to a small blue-shift in the absorbance as compared to 39.3 °C, again consistent with the weak temperature dependence of the refractive index in the isotropic phase (Figure 4).

We repeated the previous experiments using gold nanoparticles coated with decanethiol. Monolayers of decanethiol formed on continuous films of gold also cause 5CB to assume an orientation in the bulk that is parallel to the surface.[64] As shown in Figure 3c and 3d, the qualitative trends in the LSPR properties of the decanethiol functionalized gold nanoparticles are similar to the gold nanoparticles coated with hexadecanethiol. In particular, contact of the decanethiol functionalized gold nanoparticles with 5CB at room temperature led to a red-shift in the LSPR peak of 32.4 nm (550.2−582.6 nm). The larger red-shift observed with decanethiol as compared to hexadecanethiol (32.4 nm for decanethiol vs 27.1 nm for hexadecanethiol) is consistent with the predicted effects of the different thicknesses of the SAMs (and thus the proximity of 5CB to the gold).[71]

We next investigated whether the surface chemistry of the gold nanoparticles could be manipulated to influence the ordering of 5CB in the vicinity of the nanoparticles and thus the LSPR properties of the nanoparticles. We used the same gold nanoparticles that were prepared in the experiments described previously and decorated them with SAMs formed from an ethanolic solution containing a mixture of decanethiol (3.2 mM) and hexadecanethiol (0.8 mM). Past studies have established that mixed SAMs of decanethiol and hexadecanethiol formed on continuous gold films can cause bulk phases of nematic 5CB to assume an orientation that is perpendicular to the macroscopic surface.[62,64] We observed the surfaces supporting the gold nanoparticles decorated with mixed SAMs formed from decanethiol and hexadecanethiol to also cause homeotropic anchoring of 5CB. With these samples (but not others discussed below), we observed the bulk homeotropic orientation of the liquid crystal to persist from room temperature to the bulk nematic-to-isotropic transition temperature (see Supporting Information).

Following contact of 5CB with the nanoparticles decorated with the mixed SAMs, we measured the LSPR peak of the gold nanoparticles to red-shift by 27.9 nm (from 551.8 to 579.7 nm at room temperature). We next measured the temperature dependence of the LSPR peak of these gold nanoparticles. Inspection of Figure 5a reveals that between room temperature and 33.2 °C (bulk nematic-to-isotropic transition), there is little change in the LSPR properties of the nanoparticles. Surprisingly, however, the bulk transition from the nematic to the isotropic phase is also accompanied by little substantial change in the position of the LSPR absorbance maximum of the gold nanoparticles functionalized with the mixed SAM (a small red-shift of ∼0.1 nm appears to coincide with the bulk clearing temperature). Heating of 5CB above 33.2 °C leads to a gradual blue-shift in the position of the LSPR peak (see following discussion for additional data and discussion of this point). Comparison of the temperature dependence of the LSPR maxima of gold nanoparticles coated with SAMs of either hexadecanethiol or decanethiol (Figure 3) versus mixed SAMs of decanethiol and hexadecanethiol (Figure 5) reveals a qualitative difference. This result indicates that the local ordering of 5CB in the vicinity of the gold nanoparticles is influenced by their surface chemistry and that this local ordering is coupled to the LSPR properties of the system. We consider the nature of this coupling in the following paragraphs.

The ordering of the liquid crystal in the vicinity of the supported nanoparticles is a complex phenomenon, and a detailed description of the local dielectric environment requires consideration of the competing effects of the nanoparticles and glass surfaces on the ordering of the liquid crystal and requires an account of the influence of topological defects that likely form about the nanoparticles. Such a detailed description lies beyond the scope of this paper. Here, we consider a highly simplified model of the dielectric environment created by the liquid crystal near the surfaces of the nanoparticles. A more detailed description will be published elsewhere. Figure 4 plots the ordinary and extraordinary refractive indices of bulk 5CB as a function of temperature as reported by Li et al.[44] Below the nematic-

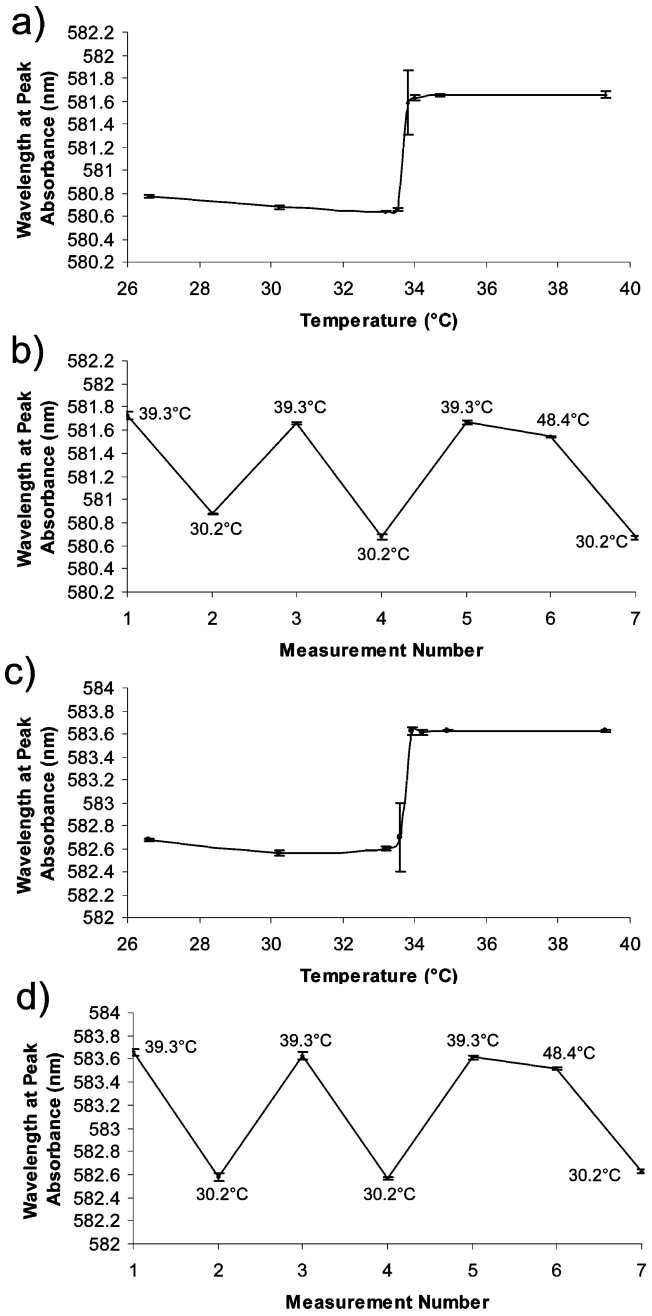

Figure 3. (a) Temperature dependence of the LSPR peak of gold nanoparticles functionalized with hexadecanethiol. The measurements were performed with the nanoparticles immersed in 5CB. Prior to chemical functionalization, the peak absorbance was measured in air to occur at 546.7 nm. (b) The same sample as in panel a as the temperature is cycled from a temperature (30.2 °C) below the isotropic−nematic transition temperature of 5CB to a temperature (39.3 °C) above the isotropic−nematic transition. The sample was heated to 48.4 °C after the third heating cycle. The plots shown in panels c and d are the corresponding plots for panels a and b obtained using a SAM formed from decanethiol. Error bars represent the standard deviation of five measurements of the same sample at the same temperature.

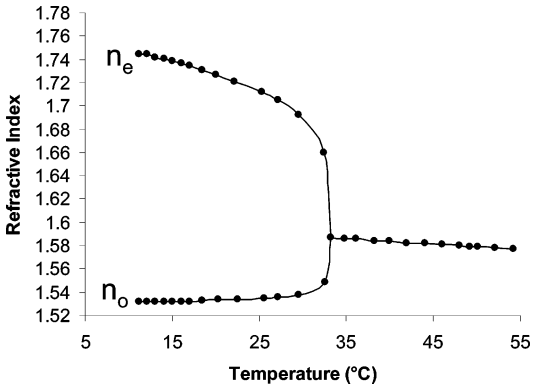

Figure 4. Ordinary (n_o) and extraordinary (n_e) refractive indices of 5CB as a function of temperature for light with a wavelength of 589 nm. Data taken from ref 44.

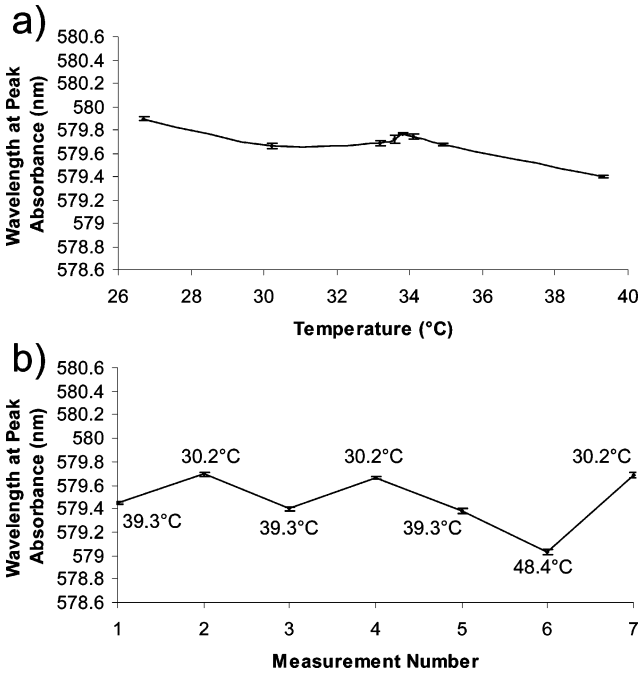

Figure 5. (a) Temperature dependence of the LSPR peak of gold nanoparticles functionalized with an 8:2 mixture of decanethiol and hexadecanethiol. The measurements were performed with the nanoparticles immersed in 5CB. Prior to chemical functionalization, the peak absorbance was measured in air to occur at 546.7 nm. (b) The same sample as in panel a as the temperature is cycled from a temperature (30.2 °C) below the isotropic−nematic transition of 5CB to a temperature (39.3 °C) above the isotropic−nematic transition. Error bars represent the standard deviation of five measurements of the same sample at the same temperature.

to-isotropic transition temperature, two refractive indices are observed, the extraordinary (larger of the two refractive indices) and ordinary refractive indices. The anisotropic optical environment defined by the liquid crystal will interact with the electromagnetic fields induced by LSPR of the nanoparticles upon illumination. These electric fields decay exponentially with distance from the surface of the nanoparticles and are known to be strongly influenced by the refractive index normal to the surface of the metal.[52,71] The simplest description of the dielectric environment experienced by the nanoparticles with the mixed SAMs is to assume that it is dominated by the extraordinary refractive index (which would exist in the case of perpendicular ordering of the liquid crystal near the surface of the nanoparticle). Similarly, as a starting point for our discussion, we consider nanoparticles functionalized with single component SAMs to experience dielectric environments that are close to the ordinary refractive index of the liquid crystal. Because the wavelength of the LSPR peak of a gold nanoparticle increases (red-shifts) with increasing refractive index of the surrounding environment, the previous physical picture leads to the prediction that the wavelength of the LSPR absorbance will be higher for nanoparticles in liquid

crystals that are functionalized with the mixed SAM as compared to the single component SAMs. This argument, however, holds true only when the distance between the metallic core of the nanoparticle and liquid crystal is constant (i.e., constant thickness of SAM on the surface of the nanoparticle). As noted previously, the mixed SAMs have a dielectric thickness that is intermediate between the pure component SAMs, and thus, interpretation of the relative position of the LSPR absorbance peaks in the liquid crystal requires consideration of both the thicknesses of the SAMs as well as the order in the liquid crystal. Our experimental observation that the wavelengths of the LSPR maxima of the nanoparticles in the liquid crystal at room temperature are 580.8 nm (hexadecanethiol coated), 582.6 nm (decanethiol coated), and 579.7 (coated with mixed SAM of hexadecanethiol and decanethiol) suggests that the effects of thickness of the SAMs on the LSPR properties of the system are indeed convolved with the effects of the ordering of the liquid crystal on the LSPR properties. This fact makes interpretation of the absolute values of the wavelengths corresponding to the LSPR difficult. However, as discussed next, examination of the temperature dependence of the LSPR peak does yield insights into the nature of the ordering of the liquid crystal about the nanoparticles.

Upon heating of 5CB from the nematic into the isotropic phase, the previous arguments lead to the prediction that nanoparticles with SAMs formed from either decanethiol or hexadecanethiol, which in the simplified model experience the ordinary refractive index of the liquid crystal, should red-shift upon heating of the liquid crystal into the isotropic phase; in contrast, the nanoparticles with mixed SAMs formed from decanethiol and hexadecanethiol should blue-shift upon heating the liquid crystal into the isotropic phase (extraordinary refractive index to isotropic refractive index). Assuming that the sensitivity of all of the SAM-modified gold nanoparticles is ∼30 nm/RIU, an increase in refractive index of ∼0.04 (characteristic of a change from the ordinary refractive index to the isotropic refractive index) at the nanoparticle surface should result in a red-shift in the LSPR peak of ∼1.2 nm. In contrast, a decrease in refractive index of ∼0.1 (extraordinary refractive index to refractive index of isotropic phase) is calculated to result in a blue-shift in the LSPR of ∼3.0 nm.

Comparison of the previous predictions to the experimental results presented in Figures 3 and 5 reveals qualitative agreement for the gold nanoparticles decorated with SAMs of either decanethiol or hexadecanethiol. The temperature dependence of the LSPR peak observed upon heating of the system into the bulk isotropic phase is consistent with transfer of the gold nanoparticles from an environment corresponding to the ordinary index of refraction of nematic 5CB to an environment of the refractive index of isotropic 5CB. Although the experimental values (0.9−1.1 nm) of the red-shifts in the LSPR peaks are similar to the calculated value of 1.2 nm, given the primitive nature of the physical model underlying our predictions, we speculate that this level of quantitative agreement is fortuitous. In contrast, the position of the LSPR peak of the nanoparticles functionalized with mixed SAMs formed from decanethiol and hexadecanethiol does not follow the temperature dependent behavior predicted for gold nanoparticles transferred from a dielectric environment corresponding to the extraordinary refractive index of 5CB to the refractive index of 5CB in the isotropic phase (Figure 4). We measured the transition from the bulk nematic phase to the isotropic phase at 33.2 °C to be accompanied by only a small excursion in the peak wavelength (∼0.1 nm). Furthermore, the overall blue-shift in the position of the LSPR peak over the entire temperature range investigated was only 0.3 nm, which is much less than the predicted value of 3.0 nm. These observations suggest that the temperature dependence of the local order of the liquid crystal near the nanoparticles decorated with the mixed SAMs is substantially different from the temperature dependence of the bulk order of the liquid crystal. To provide further insight into this behavior, we sought to determine the sensitivity of the local order of the liquid crystal to the size and spacing of the nanoparticles on the surface. Although the methodology used to prepare the supported nanoparticles in our study does not permit independent control over particle size and organization (the fabrication of such arrays is in progress), the method does permit the preparation of nanoparticle ensembles with varying LSPR maxima (caused by changes in both particle size and organization).

We repeated the previous experiments using gold nanoparticles with a LSPR peak at 538.1 nm (measured in air prior to the formation of SAMs). The qualitative behavior of these gold nanoparticles, when coated with SAMs formed from either hexadecanethiol or decanethiol, was similar to that shown in Figure 3 (see Supporting Information for the measurements). In contrast, when the nanoparticles were coated with mixed SAMs, we noted several differences between the gold nanoparticles with a LSPR peak at 538.1 nm and those reported in Figure 5. First, upon initial contact of the 5CB with the surface supporting the gold nanoparticles with a LSPR peak at 538.1 nm (coated with the mixed SAM), we observed that the bulk anchoring of the 5CB in its nematic phase at room temperature was not homeotropic. However, upon heating of this sample toward 33.2 °C, we observed a macroscopic orientational transition leading to homeotropic anchoring of the liquid crystal just prior (within a degree) to the bulk phase transition to the isotropic phase. We note that this bulk orientational behavior differs from that reported previously using samples with a LSPR peak at 546.7 nm, where a temperature independent, homeotropic orientation of the bulk liquid crystal was observed. Interestingly, we also observed differences in the temperature dependent LSPR behaviors of the two sets of nanoparticles in contact with the liquid crystal. Figure 6a shows the wavelength of the LSPR peak as a function of temperature for the second sample of nanoparticles decorated with mixed SAMs formed from hexadecanethiol and decanethiol (in contact with 5CB). In comparison to Figure 5a, the position of the LSPR peak in Figure 6a is more strongly dependent on temperature. At temperatures below 32 °C and above 34 °C, there is an overall blue-shift of 0.8 nm in the wavelength of the LSPR peak with increasing temperature. In addition, over an intermediate range of temperatures that encompasses the previously mentioned macroscopic anchoring transition of

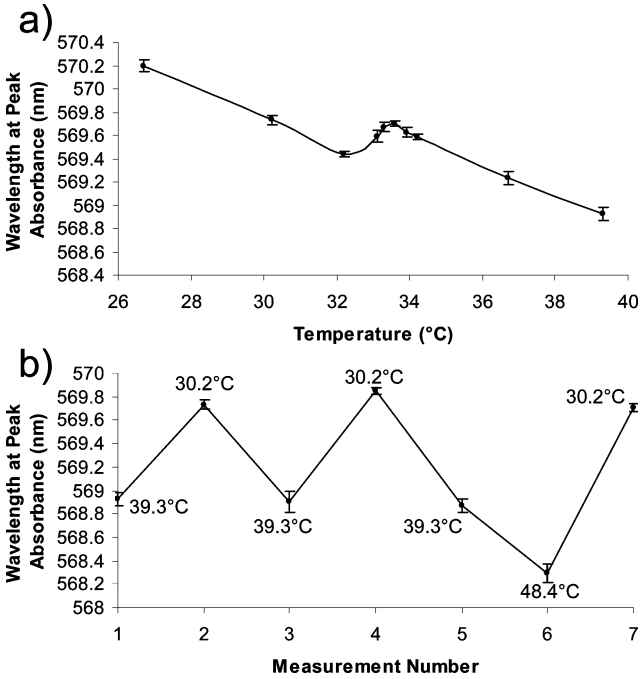

Figure 6. (a) Temperature dependence of the LSPR peak of gold nanoparticles functionalized with an 8:2 mixture of decanethiol and hexadecanethiol. The measurements were performed with the nanoparticles immersed in 5CB. Prior to chemical functionalization, the peak absorbance was measured in air to occur at 538.1 nm. (b) The same sample as in panel a as the temperature is cycled from a temperature (30.2 °C) below the isotropic−nematic transition of 5CB to a temperature (39.3 °C) above the isotropic−nematic transition. Error bars represent the standard deviation of five measurements of the same sample at the same temperature.

the liquid crystal from the parallel-to-homeotropic orientation, the position of the LSPR red-shifts with increasing temperature. This result is an interesting one because it suggests that the LSPR behavior of the nanoparticles reports nanoscopic changes in the ordering of the liquid crystal in the vicinity of the nanoparticles that underlies the macroscopic anchoring transition. We note that inspection of Table 1 reveals that the differences in the LSPR behaviors in liquid crystal reported in Figures 5 and 6 cannot be explained by the relative sensitivities of the nanoparticle arrays to their dielectric environments (as reflected in the magnitudes of the shifts in the LSPR peaks upon formation of the SAMs). Comparison of Figures 5 and 6 illustrates the dependence of the local order of the liquid crystal on the size and organization of the nanoparticles on the surface.

Although ongoing studies seek to elucidate the detailed origin of the temperature dependence of the LSPR peak measured in the previously described experiments using mixed SAMs, here we make several comments regarding the possible origin of these effects. First, we contrast our observations to the results of a recent experimental study of the effects of electric field-induced orientational transitions of bulk liquid crystals on the LSPR properties of gold nanodots (diameters of ∼75 nm; spacing ∼100 nm) supported on surfaces. In that study, the LSPR behavior of the nanodots appeared to correlate qualitatively with electric field-induced transitions in the bulk orientation of the liquid crystal.[53] In contrast, in our study of surface-induced orientational transitions, we have observed that changes in the bulk order of the liquid crystal are not always accompanied by changes in the LSPR properties of the nanoparticles. For example, as shown in Figure 5, the bulk nematic-to-isotropic transition is not accompanied by a substantial change in the wavelength of the peak absorption associated with the LSPR of the nanoparticles. From this result, we infer that the temperature dependence of the local order of the liquid crystal near the nanoparticles is substantially different from the bulk liquid crystal. We also observe, however, that changes in surface chemistry of the nanoparticles can lead to situations (Figure 6) where there does appear to be a correlation between the temperature dependence of the local and bulk ordering of the liquid crystal. For the former case (nanoparticles with mixed SAMs formed from hexadecanethiol and decanethiol), we can envisage several physical models of the local surface ordering of the liquid crystal that are consistent with our experimental observations. One model is based on the proposal that the local ordering of 5CB near the nanoparticles is preserved even after the bulk liquid crystal has melted. Local surface-induced ordering of liquid crystals has been reported previously to occur above bulk clearing temperatures.[75] A second possible model that can describe the LSPR behavior of the nanoparticles with the mixed SAMs is based on a surface-induced melting of the liquid crystal below the bulk nematic-to-isotropic transition temperature. The gold nanoparticles immobilized on the glass substrates define a rough surface, and surface roughness can decrease the local surface order of a liquid crystal as compared to the bulk,[76,77] even to the extent of local melting.[78,79] The reduced local order does not necessarily change the bulk alignment,[80,81] which would be consistent with our observations of homeotropic alignment on the nanoparticle-decorated surfaces (see Supporting Information). The consequences of localized disordering have been investigated by Chiccoli et al. using Monte Carlo simulations of a polymer fiber in a nematic liquid crystal.[81] In that study, it was found that local order that was either greater than or less than the bulk order could result in the same alignment of the liquid crystal far from the surface of the fiber. The formation of defects in the liquid crystal was also described in this study and others,[82] as well as changes in the structure of the defects with temperature. Such considerations will likely be necessary to develop a quantitative description of the LSPR behaviors that we have observed in our experiments with nanoparticles on surfaces.

Our experimental results also reveal that the size and organization of the ensemble of gold nanoparticles, in addition to the surface chemistry of the individual nanoparticles, impacts the LSPR behaviors as well as bulk orientations of the liquid crystal. We note that the functionalized gold nanoparticles supported on glass defines a microscopi-

(75) Chen, W.; Feller, M. B.; Shen, Y. R. *Phys. Rev. Lett.* **1989**, *63*, 2665.
(76) Ondris-Crawford, R. J.; Crawford, G. P.; Doane, J. W.; Zumer, S.; Vilfan, M.; Vilfan, I. *Phys. Rev. E* **1993**, *48*, 1998.
(77) Barberi, R.; Durand, G. *Phys. Rev. A* **1990**, *41*, 2207.
(78) Barbero, G.; Durand, G. *J. Phys. II* **1991**, *1*, 651.
(79) Papanek, J.; Martinot-Lagarde, P. *J. Phys. II* **1996**, *6*, 205.
(80) Wu, S. T.; Efron, U. *Appl. Phys. Lett.* **1986**, *48*, 624.
(81) Chiccoli, C.; Pasini, P.; Skacej, G.; Zannoni, C.; Zumer, S. *Phys. Rev. E* **2002**, *65*, 51703.
(82) Hung, F. R.; Guzman, O.; Gettelfinger, B. T.; Abbott, N. L.; de Pablo, J. J. *Phys. Rev. E* **2006**, *74*, 11711.

cally inhomogeneous substrate, which can result in near-surface regions of liquid crystal in which the ordering of the liquid crystal is substantially different from the bulk.[45,74] Interestingly, such interfacial regions brought about by inhomogeneous substrates can persist well above the bulk nematic-to-isotropic clearing temperature.[45,75] Ensembles of immobilized nanoparticles with long-range order are currently under investigation to understand how neighboring particles affect ordering of the liquid crystals near nanoparticle surfaces and the associated changes in LSPR properties.

Conclusion

In summary, this paper reports an experimental investigation of the LSPR properties of chemically functionalized gold nanoparticles in contact with a liquid crystal. The results presented in this paper reveal that the ordering of liquid crystals near the surfaces of gold nanoparticles can be coupled to the LSPR of the nanoparticles and that the nature of this coupling depends strongly on the surface chemistry of the gold nanoparticles. For nanoparticles functionalized with monolayers formed from either decanethiol or hexadecanethiol, the temperature dependence of the LSPR properties of the gold nanoparticles correlates closely with changes in the bulk order of the liquid crystal. In contrast, however, the LSPR properties of nanoparticles functionalized with SAMs formed from mixed monolayers of decanethiol and hexadecanethiol reveal that the localized order of the liquid crystal in the vicinity of the nanoparticles does not change with temperature in a manner that correlates closely with the bulk liquid crystal. With this latter class of chemically functionalized nanoparticles, the local ordering of the liquid crystal in the vicinity of the nanoparticles, as inferred from the LSPR behavior, was dependent on the sizes of the nanoparticles and/or organization of the ensemble of nanoparticles. The above results, when combined, suggest that investigations of the LSPR properties of nanoparticles immersed in liquid crystals can be used to characterize the local ordering of liquid crystals in the vicinity of nanoparticles. In addition, the coupling between the order of the liquid crystal and the LSPR properties of the nanoparticles suggests the basis of novel approach for the formation of active optical nanostructures including nanostructures capable of chemical sensing.[83]

Acknowledgment. This research was partially supported by the University of Wisconsin, Nanoscale Science and Engineering Center (NSEC, DMR-0425880), by DMR-0602570, and by the Army Research Office W911NF-06-1-0314.

Supporting Information Available: Effects of isotropic solvents on the LSPR properties of the gold nanoparticles, polarized light micrographs of liquid crystals, and LSPR properties of gold nanoparticles with an initial absorbance maximum of 538.1 nm. This material is available free of charge via the Internet at http://pubs.acs.org.

CM062438P

(83) Shah, R. R.; Abbott, N. L. *Science* **2001**, *293*, 1296.